OPEN

Evodiamine inhibits vasculogenic mimicry in HCT116 cells by suppressing hypoxia-inducible factor 1-alpha-mediated angiogenesis

Di Zeng[a], Peng Zhou[a], Rong Jiang[a], Xiao-peng Li[a], Shi-ying Huang[a], Dan-yang Li[a], Guo-li Li[a], Li-sha Li[a], Shuang Zhao[a], Ling Hu[b], Jian-hua Ran[b], Di-long Chen[a,c], Ya-ping Wang[a] and Jing Li[a]

Evodiamine (Evo), a quinazoline alkaloid and one of the most typical polycyclic heterocycles, is mainly isolated from *Evodia rugulosa*. Vasculogenic mimicry (VM) is a newly identified way of angiogenesis during tumor neovascularization, which is prevalent in a variety of highly invasive tumors. The purpose of this study was to investigate the effect and mechanism of Evo on VM in human colorectal cancer (CRC) cells. The number of VM structures was calculated by the three-dimensional culture of human CRC cells. Wound-healing was used to detect the migration of HCT116 cells. Gene expression was detected by reverse transcription-quantitative PCR assay. CD31/ PAS staining was used to identify VM. Western blotting and immunofluorescence were used to detect protein levels. The results showed that Evo inhibited the migration of HCT116 cells, as well as the formation of VM. Furthermore, Evo reduced the expression of hypoxia-inducible factor 1-alpha (HIF-1α), VE-cadherin, VEGF, MMP2, and MMP9. In a model of subcutaneous xenotransplantation, Evo also inhibited tumor growth and VM formation. Our study demonstrates that Evo could inhibit VM in CRC cells HCT116 and reduce the expression of HIF-1α, VE-cadherin, VEGF, MMP2, and MMP9.

Anti-Cancer Drugs 2021, **32**:314–322

Keywords: colorectal cancer, Evodia, evodiamine, hypoxia-inducible factor 1-alpha, vasculogenic mimicry

[a]Department of Histology and Embryology, Chongqing Medical University, [b]Department of Anatomy, Neuroscience Research Center, Chongqing Medical University and [c]Engineering Research Center of Antitumor Natural Drugs, Chongqing Three Gorges Medical College, Chongqing, China

Correspondence to Jing Li, PhD, Department of Histology and Embryology, Chongqing Medical University, Chongqing 400016, China
Tel: +86 13370762980; e-mail: 100392@cqmu.edu.cn

Received 22 April 2020 **Revised form accepted** 5 December 2020

Introduction

In 2012, six cellular mechanisms for tumor angiogenesis were reviewed [1]. Among them, vasculogenic mimicry (VM) is an important one. The concept of VM is that some highly malignant tumor cells can change their shape to form a duct system and connect with blood vessels, thus allowing tumors to obtain a blood supply [2]. In recent years, VM has been identified in a variety of tumors [3].

At present, the mechanism of VM formation is not very clear. Previous studies have shown that hypoxia-inducible factor 1-alpha (HIF-1α) is highly expressed in various malignant tumor tissues and plays a key role in regulating the formation of VM [4]. Besides, vascular endothelial-cadherin (VE-cadherin), an adhesion protein, is one of the major regulators of VM formation [5]. Moreover, VE growth factor (VEGF) can strongly induce endothelial cell proliferation and tubular structure formation, and is an important factor in inducing blood vessel growth [6]. In addition, the matrix metalloproteinase (MMP) family can regulate the migration of various tumor cells in the extracellular matrix and enhance the adhesion of tumor cells, so that tumor cells can undergo angiogenesis mimicry via VM and connect with endothelium-dependent vessels [7,8]. In breast cancer cells, hypoxia can activate HIF-1α, leading to the upregulation of VE-cadherin which resulted in the rise of MMP2 and MMP9 expression levels to enhance the invasiveness and eventually leading to VM formation [9]. In melanoma, the activation of HIF-1a leads to a high expression of VEGF, resulting in the upregulation of MMPs, enabling the cells to become more invasive and form VM [10].

Evodiamine (Evo), a quinazoline alkaloid and one of the most typical polycyclic heterocycles, is mainly isolated from *Evodia rugulosa* [11]. Previous studies have shown that Evo has a variety of pharmacological activities [12]. And a study showed that in hepatocellular carcinoma, Evo exerts antitumor effects, at least in part through inhibiting the β-catenin-mediated transcription of angiogenesis factors [13]. Another study suggested that Evo is a potent inhibitor of angiogenesis, and the mechanism may probably involve repression of ERK phosphorylation in human lung adenocarcinoma cell line CL1 [14]. However, it is not clear whether Evo could inhibits the formation of VM.

0959-4973 Copyright © 2020 The Author(s). Published by Wolters Kluwer Health, Inc. DOI: 10.1097/CAD.0000000000001030

Our study investigated the effect of Evo on the formation of VM in colorectal cancer (CRC), as well as its possible mechanism.

Materials and methods

Reagents and antibodies

Evo (cat. no. S2382; purity 99.76%; Selleck Chemicals, Houston, Texas, USA) was dissolved in dimethyl sulfoxide and phosphate buffer saline (PBS), respectively. Antibodies against HIF-1α, VE-cadherin, and MMP2 were purchased from Cell Signaling Technology, Inc (Danvers, Massachusetts, USA). Antibodies against VEGF, MMP9, and Platelet endothelial cell adhesion molecule-1 (CD31) were purchased from Abcam (Cambridge, UK). The antibody against glyceraldehyde-3-phosphate dehydrogenase (GAPDH) was purchased from Bioworld Technology, Inc (Bloomington, Minnesota, USA). ML228 and PX478 were purchased from MedChemExpress, Inc. Cell Counting kit-8 was purchased from Dojindo Molecular Technologies, Inc (Kumamoto, Japan). Glycogen periodic-acid Schiff (PAS) stain kit was purchased from Beijing Solarbio Science & Technology Co., Ltd (Beijing, China).

Cell culture and culture conditions

The human CRC cell lines SW480 cells and HCT116 cells were purchased from Zhong Qiao Xin Zhou Biotechnology Company (Shanghai, China). The human umbilical vein endothelial cell line (HUVECs) was a gift from the Laboratory of Neuroscience Research Center of Chongqing Medical University. Cells were maintained in DMEM medium containing 10% fetal bovine serum (Gibco, Carlsbad, California, USA) with 100 μg/ml penicillin and streptomycin (Gibco) and incubated at 37 °C under 5% CO_2.

Tube-like structure formation assay

A total of 50 μl growth factor-reduced Matrigel (BD Biosciences, San Jose, California, USA) was added to each well of a 96-well plate and solidifying at 37 °C for 30 minutes. Cells were suspended in DMEM with or without Evo (1.5 μM) and were seeded on a 96-well plate coated with Matrigel. After 24 h of incubation, the number of tube-like structures in each group was assessed for ≥6 different fields under a light microscope.

Cell viability assay

Cell viability was detected by CCK-8 assay. HCT116 cells in the logarithmic growth phase were inoculated into a 96-well plate. After adhering, the culture supernatant was discarded and complete medium with or without Evo was added. After the cells were cultured for 24 h, 10 μl CCK-8 reagent was added to each well and incubated in a 37 °C incubator for 2 h. The absorbance of each well was measured at 450 nm by a microplate reader (Bio-Rad Laboratories, Inc., Berkeley, California, USA).

Wound-healing assay

HCT116 cells in the logarithmic growth phase were seeded in six-well plates. After the cells grew into a single layer, a sterile 10 μl pipette tip was used to draw straight scratches in the cells. The suspended cells were washed off with PBS and photographs were obtained with a microscope. Medium containing Evo at concentrations of 0 or 1.5 μM was added according to the experimental design, and after culturing for 24 h, photographs were obtained under an inverted microscope.

Reverse transcription-quantitative PCR assay

qPCR was conducted in a CFX Connect™ Real-Time PCR Detection System (Bio-Rad Laboratories, Inc.) using 1 μl cDNA and iTaq™ Universal SYBR Green Supermix (Bio-Rad Laboratories, Inc.) as recommended by the manufacturer. The relative quantification values for each gene were calculated by the $2^{-\Delta\Delta Ct}$ method using GAPDH as an internal reference. The primers used (TsingKe Biotech, Beijing, China) were as follows: HIF-1α forward 5′-ACGTTCCTTCGATCAGTTGTCACC-3′, HIF-1α reverse 5′-GGCAGTGGTAGTGGTGGCATTAG-3′; VE-cadherin forward 5′- AAAGAATCCATTGTGCA AGTCC-3′, VE-cadherin reverse 5′-CGTGTTATCGTG ATTATCCGTG-3′; VEGF forward 5′-ATCGAGTACA TCTTCAAGCCAT-3′, VEGF reverse 5′-GTGAGGTT TGATCCGCATAATC-3′; MMP2 forward 5′- ATTGTA TTTGATGGCATCGCTC-3′, MMP2 reverse 5′-ATT CATTCCCTGCAAAGAACAC-3′; MMP9 forward 5′-CAGTACCGAGAGAAAGCCTATT-3′, MMP9 reverse 5′- CAGGATGTCATAGGTCACGTAG-3′; and GAPDH forward 5′-AGAAAAACCTGCCAAATATGAT GAC-3′, GAPDH reverse 5′-TGGGTGTCGCTGTT GAAGTC-3′.

Xenograft models in nude mice

BALB/c nude mice (female, 6 weeks old) were purchased from the Laboratory Animal Center of Chongqing Medical University. HCT116 cells (1×10^7 cells/ml, ~0.2 ml) were subcutaneous injected into the right armpit of the BALB/c nude mice. After the tumor grew to 0.5 cm in diameter, 20 mice were randomly divided into two groups: 10 in the Evo group and 10 in the control group. Evo (10 mg/kg) was administered with a gavage needle once a day, while the control group was treated with normal saline. The tumor volume was calculated using the formula tumor volume = $(\text{width})^2 \times \text{length}/2$. After 22 days, the mice were sacrificed by cervical dislocation. All animal experiments were approved by the Animal Experimental Center of Chongqing Medical University and carried out in accordance with the principles of laboratory animal care.

Immunoblot assay

Tumor cells or homogenized tumor samples were lysed on ice in a lysis buffer containing 1%

Fig. 1

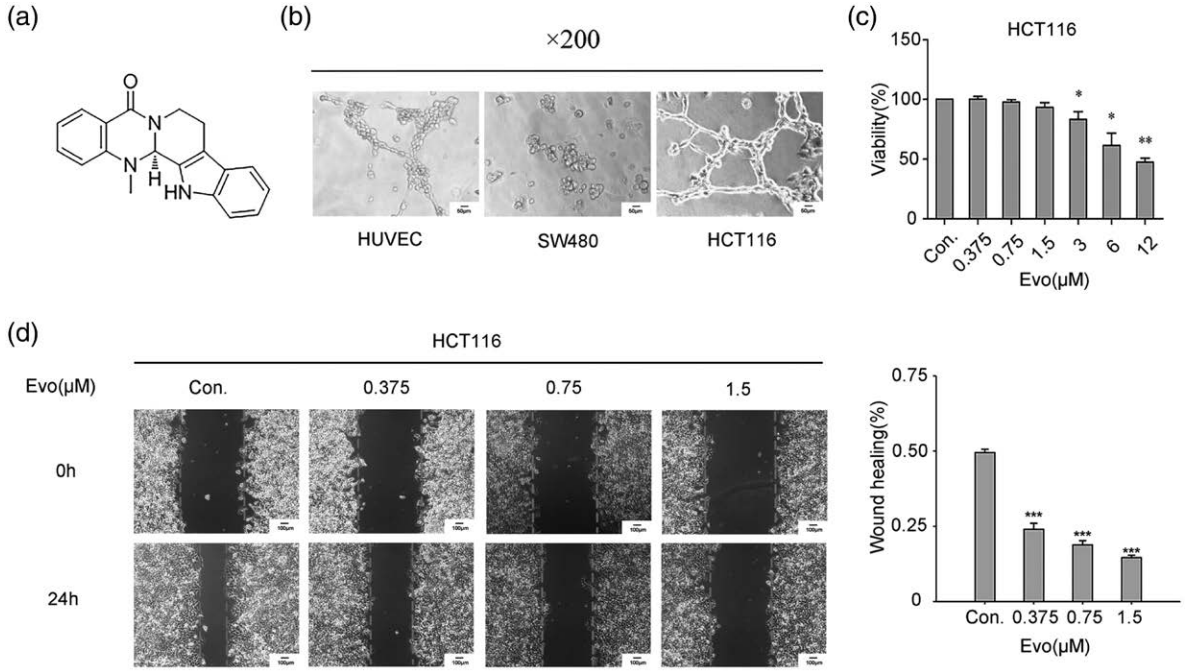

HCT116 cells can display VM, and Evo inhibits cell migration *in vitro*. (a) Chemical structure of Evo. (b) Tube formation assays were performed in HUVECs (left), SW480 cells (middle), and HCT116 cells (right) in three-dimensional culture on a Matrigel matrix, and the morphology of the cells was observed (magnification, ×200). (c) HCT116 cells were treated with different concentrations of Evo for 24 h, and cell viability was measured by CCK-8 assay. (d) Wound-healing assay. The migration rate of HCT116 cells under treatment with Evo for 24 h was detected. Data represent the mean ± SD. Each group was a mixture of cells collected three times and all experiments were performed in triplicate. $^{*}P < 0.05$, $^{**}P < 0.01$, $^{***}P < 0.001$ vs. control. HUVECs, human umbilical vein endothelial cell line; VM, vasculogenic mimicry.

phenylmethanesulfonylfluoride for 30 minutes. After centrifugation, the supernatant was collected. Protein concentration was determined using a BCA Protein Assay kit (Beyotime Institute of Biotechnology, Shanghai, China). The proteins were subjected to SDS-PAGE. Then, the separated proteins were transferred to a polyvinylidene difluoride membrane. Next, the membranes were blocked with 5% nonfat milk for 1 h, and the corresponding primary antibody was added, followed by overnight incubation at 4 °C. Then the corresponding secondary antibody was added and incubated for 1 h at room temperature. GAPDH was used as the loading control. ChemiDoc Touch Imaging System (Bio-Rad Laboratories, Inc.) was used to develop the immunoblots.

Immunofluorescence staining

HCT116 cells were fixed in 4% paraformaldehyde. Next, the cells were permeabilized with PBS containing 0.5% Triton X-100 for 30 minutes. The cells were fixed with 1% goat serum albumin blocking solution for 30 minutes. Next, primary antibodies were added and incubated at 4 °C overnight. Then the cells were stained with the secondary antibody for 1 h at 37 °C. The nuclei were stained with DAPI for 5 minutes. Optimal cutting temperature compound was added to embed the tissues at –21 °C for 10 minutes. Sections of frozen tissue were immobilized with cold acetone for 10 minutes and soaked in a PBS solution twice. For immunofluorescence staining, the specific treatment applied was the same that employed in cell immunofluorescence staining. Images were captured with a laser confocal microscope (Nikon Corp., Tokyo, Japan).

Immunohistochemistry and CD31/periodic-acid Schiff double staining

Immunohistochemistry staining was performed using the Immunohistochemistry Sp 9000 kit (Zhongshan Chemical, Beijing, China). According to the manufacturer's instructions, after overnight incubation with rabbit anti-CD31 primary antibody at 4 °C, the cells were rewarmed for 30 minutes in a water bath, and the secondary antibody was applied to the water bath for 30 minutes. The sections were then incubated with streptavidin-HRP for 30 minutes at room temperature. A diaminobenzidine solution was added to develop the color, followed by PAS staining according to the manufacturer's instructions.

Statistical analysis

Figures in the text are representative of at least three independent experiments. All the data were presented as mean ± SD. Statistical analysis was performed using

Fig. 2

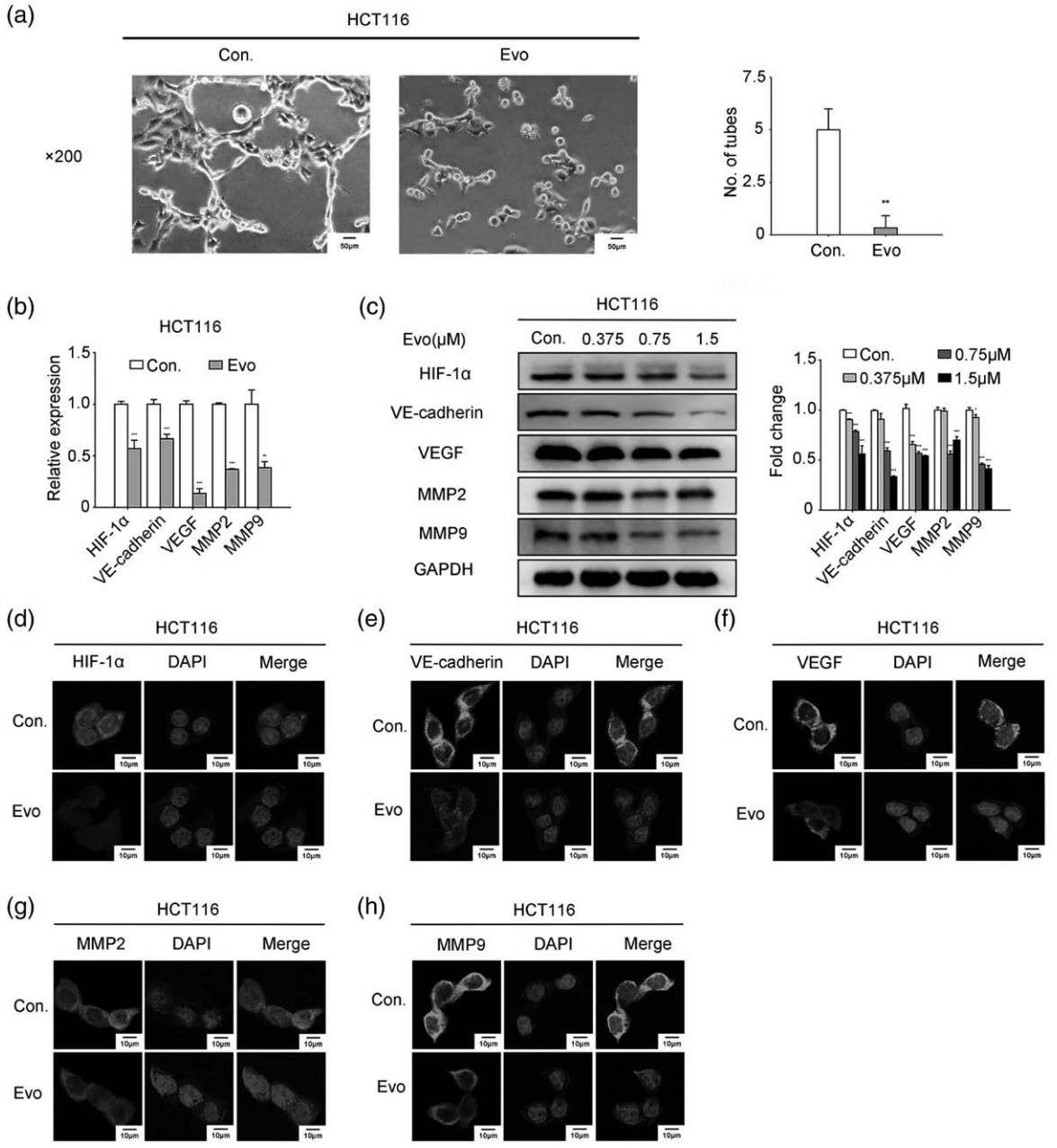

Evo inhibits the formation of VM and down-regulates the level of proteins related to VM formation. (a) Effect of Evo (1.5 μM) on the formation of VM in HCT116 cells. Magnification, ×200. (b) The expression of HIF-1α, VE-cadherin, VEGF, MMP2, and MMP9 in HCT116 cells was detected by RT-qPCR assay. (c) HCT116 cells were incubated with or without Evo (0, 0.375, 0.75, and 1.5 μM) for 24 h. Western blot assay was performed to detect protein levels. (d–h) Representative immunofluorescence images (magnification, ×400). HCT116 cells were incubated with or without Evo (0 and 1.5 μM) for 24 h to detect the levels of HIF-1α, VE-cadherin, VEGF, MMP2, and MMP9. Data represent the mean ± SD. Each group was a mixture of cells collected three times and all experiments were performed in triplicate. $^{*}P < 0.05$, $^{**}P < 0.01$, $^{***}P < 0.001$ vs. control. RT-qPCR, reverse transcription-quantitative PCR; VEGF, vascular endothelial growth factor; VM, vasculogenic mimicry.

SPSS version 22.0 (IBM Corp, Armonk, New York, USA). Repetitive measure analysis of variance (ANOVA) was used in analyzing the tumor volume at different time points. Other data were analyzed by one-way ANOVA, followed by *t*-tests. $P < 0.05$ was considered statistically significant.

Results

HCT116 cells can display vasculogenic mimicry, and Evo inhibits cell migration *in vitro*

The chemical structure of Evo ($C_{19}H_{17}N_3O$) is shown in Fig. 1a. As presented in Fig. 1b, tube-like structure was found in HUVECs (left).VM was not observed in SW480

cells (middle). However, VM was common in HCT116 cells (right). HCT116 cells were treated with different concentrations of Evo (0, 0.375, 0.75, 1.5, 3, 6, and 12 μM) for 24 h. Cell viability was detected by CCK-8 assay. The viability of HCT116 cells was significantly affected by Evo (3, 6, and 12 μM) (Fig. 1c), but when the cells were treated with Evo (0.375, 0.75, and 1.5 μM) for 24 h, >90% of the cells survived, and compared with the control group, the difference was not statistically significant. To ensure that the cell viability is as free as possible from drug inhibition, cells were treated with these low concentrations of drugs in subsequent experiments. The wound-healing assay showed that the Evo treatment group had a lower wound-healing rate; thus, Evo can inhibit the migration of HCT116 cells (Fig. 1d).

Evo inhibits the formation of vasculogenic mimicry and down-regulates the level of proteins related to vasculogenic mimicry formation

The formation of VM in HCT116 cells was affected by Evo. After treatment with Evo (1.5 μM) for 24 h, the number of tubes was significantly decreased compared with that in the untreated group ($P < 0.001$) (Fig. 2a). As shown in Fig. 2b, the reverse transcription-quantitative PCR results showed that compared with that in the control group, the expression of HIF-1α, VE-cadherin, VEGF, MMP2, and MMP9 was significantly decreased in HCT116 cells after treatment with Evo (1.5 μM) for 24 h. Furthermore, western blot assay was applied to detect the protein levels of HIF-1α, VE-cadherin, VEGF, MMP2, and MMP9 in HCT116 cells. The protein levels significantly decreased in a concentration-dependent manner after Evo treatment compared with those in the control group (Fig. 2c). Besides, the immunofluorescence results showed that compared with that in the control group, the level of HIF-1α, VE-cadherin, VEGF, MMP2, and MMP9 was significantly decreased in HCT116 cells after treatment with Evo (1.5 μM) for 24 h. (Fig. 2d–h). Consequently, Evo inhibited the formation of VM and decreased the expression of HIF-1α, VE-cadherin, VEGF, MMP2, and MMP9.

Evo inhibits the formation of vasculogenic mimicry and its possible mechanism

HIF-1α plays a key role in VM formation in tumor cells. To further verify this point and study the effect of Evo, HCT116 cells were treated with Evo, ML228 (an agonist of HIF-1α), Evo + ML228, PX478 (an inhibitor of HIF-1α), or Evo + PX478 (Fig. 3a). The results showed that, in the ML228 group, the number of tubes increased significantly. The combination treatment of Evo and ML228 can weaken the enhancement effect of agonists for forming tubes. In the Evo, PX478, and Evo + PX478 groups, the number of tubes decreased obviously. Also, western blot assay was performed to detect the levels of proteins. The results showed that Evo inhibited the expression of HIF-1α, VE-cadherin, VEGF, MMP2, and MMP9. Moreover, ML228 could up-regulate the levels of these proteins, while PX478 could down-regulate the levels of these proteins. Besides, in the Evo + ML228 and the Evo + PX478 groups, Evo attenuated the upregulation of these proteins by ML228 and enhanced the downregulation of these proteins by PX478 (Fig. 3b and c). Therefore, Evo could suppress HIF-1α, leading to the downregulation of VE-cadherin and VEGF which resulted in the decrease of MMP2 and MMP9 expression levels to reduce the invasiveness and VM formation.

Evo inhibits HCT116 cell growth and vasculogenic mimicry formation *in vivo*

At the beginning of the experiment, the body weight of the mice on the control group (17.04 ± 0.38 g, mean ± SD) was similar to Evo group (16.87 ± 0.32 g). At time of sacrifice, the body weight of the mice on the control group (19.45 ± 0.72 g) was similar to Evo group (19.51 ± 0.65 g). There was no significant difference in mouse body weight between the control and Evo groups, suggesting that Evo treatment did not cause significant systemic toxicity (Fig. 4a). The results showed that Evo treatment inhibited tumor growth *in vivo*, as demonstrated by the smaller tumor size in Evo-treated mice (Fig. 4b and c). Besides, hematoxylin and eosin staining revealed that, in the control group, the tumor cells in the tumor tissues were rich and disordered; the cells were polygonal; nuclear atypia was obvious; and there were more pathological mitotic figures, less nuclear pyknosis, and smaller flaky necrotic area than in the Evo-treated group. In the Evo-treated group, the tumor cells in the tumor tissues were fusiform and round; the cells were shrunk; the nucleus was strongly stained; and the mitotic figures were significantly reduced; scattered focal and flaky necrosis was observed (Fig. 4d). VM was examined by CD31/PAS double staining (Fig. 4e). $CD31^+/PAS^+$ represented endothelium-dependent vessels (up), while $CD31^-/PAS^+$ represented VM (down) (magnification, ×400). Decreased VM count was observed in the Evo-treated group (Fig. 4f). The VM channel was composed of tumor cells, and CD31 was negative (red arrow; magnification, ×200), while endothelium-dependent vessels were both CD31- and PAS-positive (black arrow; magnification, ×200). The results showed that, compared with that of the control group, the number of $CD31^-/PAS^+$ channels in the Evo group decreased significantly, and the VM forming ability decreased.

Possible molecular mechanism of Evo antitumor vasculogenic mimicry effect *in vivo*

As shown in Fig. 5a, the protein levels of HIF-1α, VE-cadherin, VEGF, MMP2, and MMP9 were decreased in the experimental mice compared with those in the control mice. Tumors were analyzed by immunofluorescence to investigate the levels of proteins. There were decreases in the levels of HIF-1α, VE-cadherin, VEGF, MMP2, and MMP9 in xenografted tumors of mice

Fig. 3

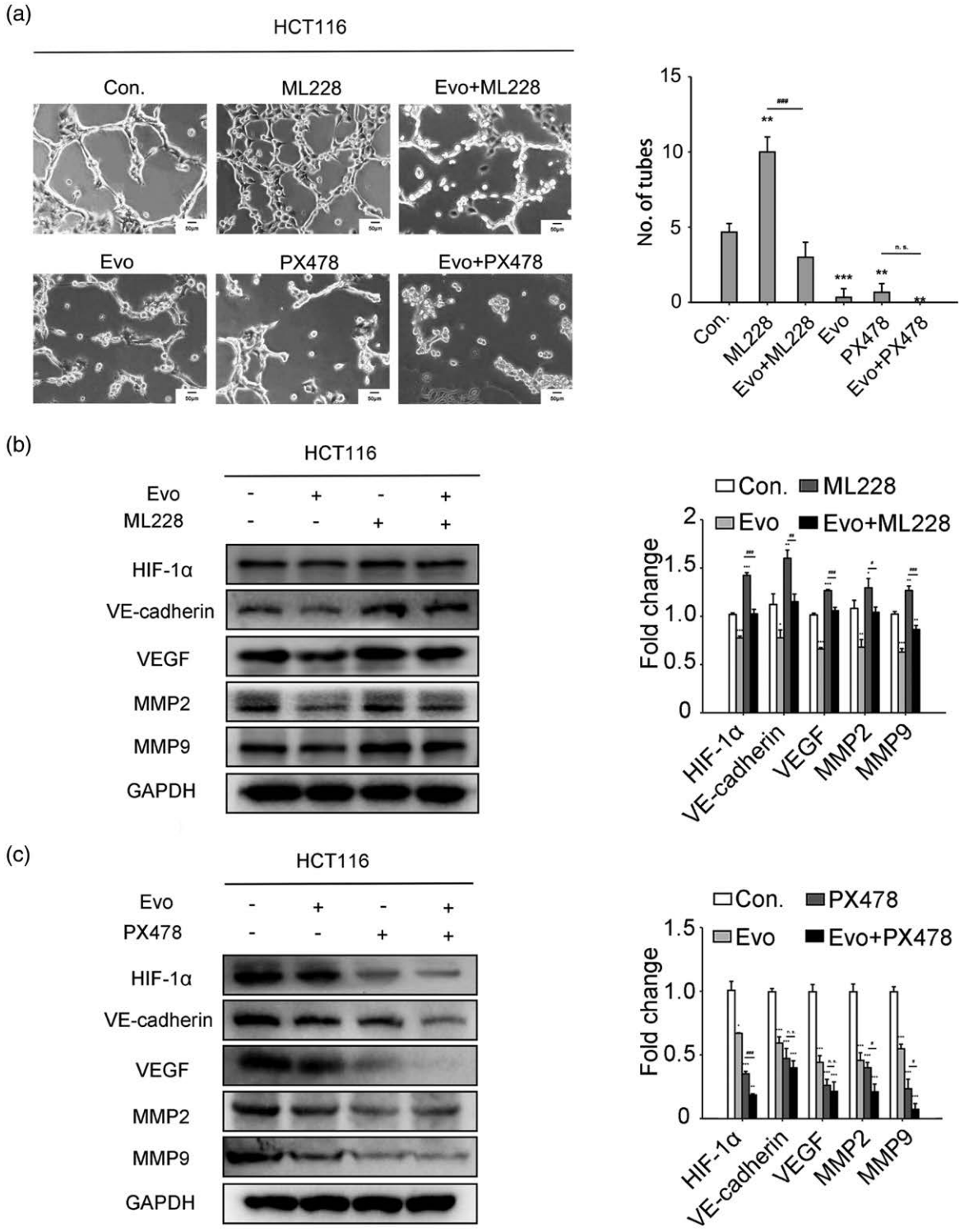

Evo inhibits the formation of VM and its possible mechanism. (a) Tube formation assays were performed in HCT116 cells treated with or without Evo, ML228, Evo + ML228, PX478, or Evo + PX478 (magnification, ×200). (b) HCT116 cells were incubated with Evo, ML228, or Evo + ML228. Western blot assay was performed to detect protein levels. (c) HCT116 cells were incubated with Evo, PX478, or Evo + PX478. Western blot assay was performed to detect protein levels. Data represent the mean ± SD. Each group was a mixture of cells collected three times and all experiments were performed in triplicate. *$P < 0.05$, **$P < 0.01$, ***$P < 0.001$ vs. control; #$P < 0.05$; ##$P < 0.01$; ###$P < 0.001$. VM, vasculogenic mimicry.

Fig. 4

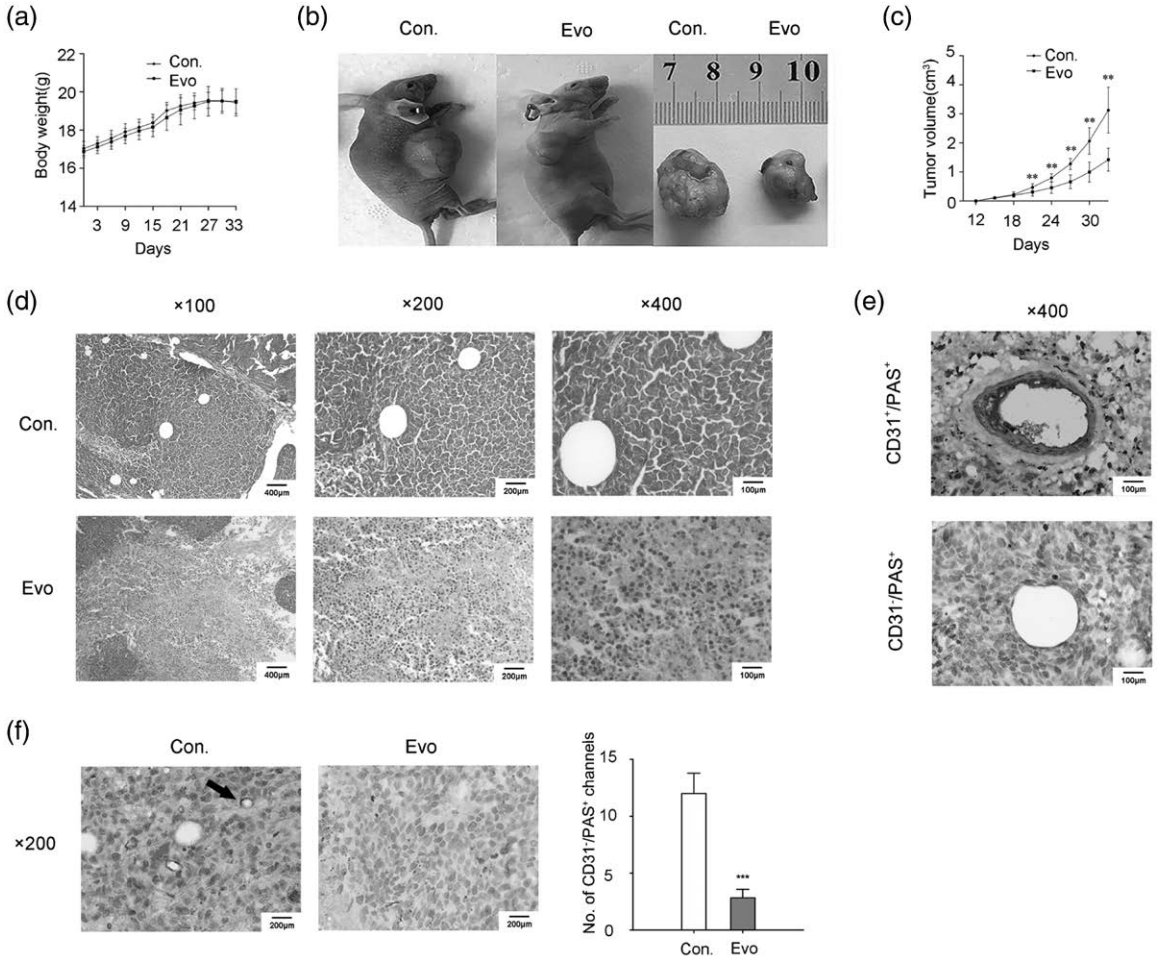

Evo inhibits HCT116 cell growth and VM formation *in vivo*. (a) Mice body weights were recorded and compared. (b) Representative images of the tumor in the control and Evo treatment groups. (c) Tumor volumes were recorded and compared at the end of the experiment when the mice were sacrificed by dislocation after anesthesia. (d) Xenograft tumor tissues were analyzed for hematoxylin and eosin staining (magnification, ×100, ×200, and ×400). (e) VM was detected with CD31/PAS double staining. $CD31^+/PAS^+$ indicated endothelial-dependent vessels (up), while $CD31^-/PAS^+$ indicated VM (down) (magnification, ×400). (f) The VM channels are lined with tumor cells (red arrows; CD31/PAS double staining; magnification, ×200). The endothelial-dependent vessels are both positive for CD31 and PAS (black arrows; CD31/PAS double staining; magnification, ×200). Data represent the mean ± SD ($n = 10$/group). All experiments were performed in triplicate. $^*P < 0.05$, $^{**}P < 0.01$ vs. control. PAS, periodic-acid Schiff; VM, vasculogenic mimicry.

treated with Evo, which was consistent with the data *in vitro* (Fig. 5b–f).

Discussion

Recent studies have identified a new type of tumor blood supply pattern, which is not dependent on angiogenesis but VM [2]. To study the role of VM in CRC, HUVEC (the positive control), the CRC cell lines SW480 and HCT116 were cultured in a three-dimensional culture system *in vitro*. We found that both HUVEC cells and HCT116 cells can form a typical tubular structure in the culture system, while SW480 cells could not (Fig. 1b). Consequently, HCT116 cells were selected for subsequent experiments. Next, a model of tumor xenograft in nude mice with HCT116 cells was constructed, and the presence of VM was detected by CD31/PAS double staining. The results revealed that VM exists in highly metastatic CRC (Fig. 4e and f).

Due to the presence of VM, traditional anti-angiogenesis therapy, which targets endothelial-dependent vessels, did not achieve the desired effect, as the tumor can still obtain blood supply from VM, in which case the combination with anti-VM treatment should be considered [15]. A previous study of our team proved that Evo inhibits migration and invasion by Sirt1-mediated post-translational modulations in CRC [16]. Also, Evo could inhibit tumor growth and metastasis by blocking the cell cycle and inhibiting infiltration [17]. This study showed that Evo inhibited the migration of HCT116 cells, as well as the formation of VM *in vitro* and *in vivo* (Figs. 1d and f and 2a), and indicated that Evo had the potential to act as an anti-VM agent.

Fig. 5

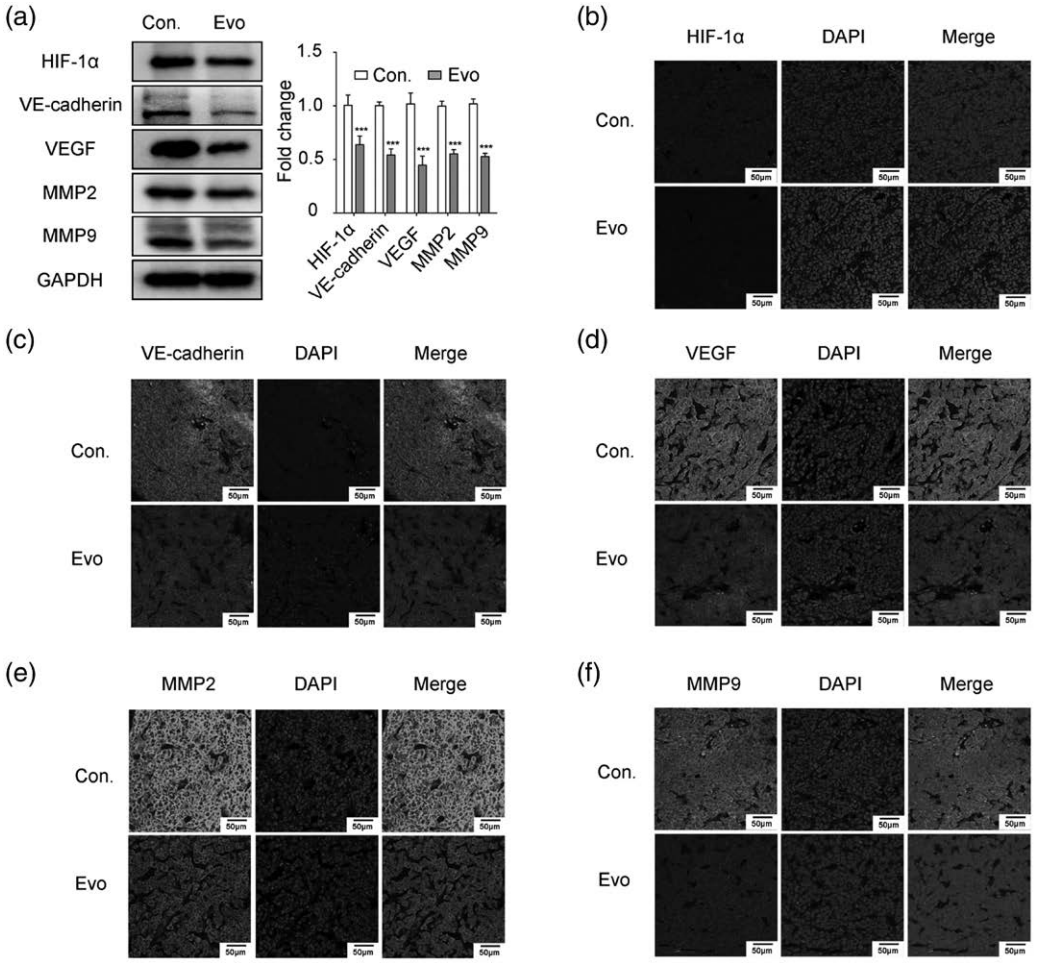

Possible molecular mechanism of Evo antitumor VM effect *in vivo*. (a) Mice were treated with or without 10 mg/kg Evo. The levels of proteins in tumor tissues were detected by western blotting. (b–f) Representative immunofluorescence images. Expression of HIF-1α, vascular endothelial-cadherin, vascular endothelial growth factor, MMP2, and MMP9 in tumor tissues was analyzed by immunofluorescence (magnification, ×400). Data represent the mean ± SD ($n = 10$/group). All experiments were performed in triplicate. *$P < 0.05$, **$P < 0.01$, ***$P < 0.001$ vs. control. VM, vasculogenic mimicry.

At present, the specific mechanism of VM formation is not fully clear. The formation of VM is associated with some key factors, such as HIF-1α, VE-cadherin, VEGF, and MMPs. A previous study showed that Epstein–Barr virus infection-induced VM and HIF-1α activation [4]. Specific reduction of VE-cadherin expression can significantly inhibit the formation of VM [18]. VM formation in gastric cancer cells was inhibited by suppressing VEGF [19]. In malignant melanoma cells, the application of anti-MMPs antibodies weakened the formation of VM [20]. Our western blot and immunofluorescence staining results showed that Evo could decrease the expression of HIF-1α, VE-cadherin, VEGF, MMP2, and MMP9 *in vitro* and *in vivo* (Figs. 2b–d and 5a–f).

Furthermore, in the hypoxic environment of the internal tumor mass, which is regulated by oxygen partial pressure, HIF-1α is activated, further promoting the expression of multiple genes involved in the process of angiogenesis [21]. HIF-1α can regulate the expression of VEGF and VE-cadherin. VEGF relates to vascular permeability, and VE-cadherin helps to maintain the stability of vascular structure stable [5,6]. MMP2 regulates the migration of various tumor cells in the extracellular matrix through integrin and enhances fibronectin-mediated tumor cell adhesion [7], and MMP9 can effectively affect the vascularization and growth rate of tumor cells, and the formation and degradation of cell-matrix in the tumor microenvironment [8]. Therefore, it was hypothesized that the formation of VM in HCT116 cells may be mediated by the hypoxia regulatory effect of HIF-1α, which activates VE-cadherin, VEGF, and MMPs. Our results showed that Evo decreased the expression of HIF-1α, thus leading to the inhibition of VE-cadherin, VEGF, MMP2, and MMP9. And the results showed that in the ML228 group, the number of VM tubes increased significantly. The combination treatment of Evo and

ML228 can weaken the enhancement effect of agonists for forming tubes. In the Evo, PX478, and Evo + PX478 groups, the number of tubes decreased obviously. ML228 could weaken the downregulation of HIF-1α, VE-cadherin, VEGF, MMP2, and MMP9 protein levels. By contrast, PX478 could enhance the downregulation of the protein levels (Fig. 3a–d). These findings suggest that Evo plays an anti-VM formation role in CRC, and the possible mechanism may be related to the inhibition of HIF-1α-mediated angiogenesis.

In addition, Pigment Epithelium Derived Factor (PEDF) is a potent endogenous inhibitor of angiogenesis, which could activate downstream signaling events inside the cell through binding to its receptors, further inhibiting the growth of a wide variety of cancer types [22]. PEDF knockdown in poorly aggressive melanoma cell lines augmented VM [23]. Endostatin, thrombospondins-1 (TSP-1), and angiostatin were recognized as the primary anti-angiogenic factors [24]. Studies have shown that endostatin suppressed angiogenesis in remote metastases by counteracting the angiogenesis genes up-regulated by VEGF, leading to regression of tumor [25]. And recombinant human endostatin combined with radiotherapy significantly inhibited the VM of human esophageal cancer cells [26]. Researchers speculated that TSP-1 may function as a tumor vascular promoting factor during melanoma VM [27]. But so far, no direct evidence has been found to show that TSP can regulate VM formation. Also, the effects of Evo on PEDF, endostatin, TSP-1, and angiostatin have not been reported by researchers. Then, can Evo inhibit the formation of VM by regulating other genes related to angiogenesis?

Conclusion

We first proposed that Evo could prevent the formation of VM in CRC, which may be associated with the inhibition of HIF-1α, leading to the downregulation of VE-cadherin and VEGF which resulted in the decrease of MMP2 and MMP9 expression level to reduce the invasiveness. However, the formation of VM is a complicated process. Whether Evo can regulate this process through other mechanisms is worth exploring in the future.

Acknowledgements

This work was supported by the National Natural Science Foundation of China (grant no. 31271368).

Conflicts of interest

There are no conflicts of interest.

References

1 Jain RK, Carmeliet P. SnapShot: tumor angiogenesis. *Cell* 2012; **149**:1408–1408.e1.
2 Maniotis AJ, Folberg R, Hess A, Seftor EA, Gardner LM, Pe'er J, *et al*. Vascular channel formation by human melanoma cells *in vivo* and *in vitro*: vasculogenic mimicry. *Am J Pathol* 1999; **155**:739–752.
3 Williamson SC, Metcalf RL, Trapani F, Mohan S, Antonello J, Abbott B, *et al*. Vasculogenic mimicry in small cell lung cancer. *Nat Commun* 2016; **7**:13322.
4 Xiang T, Lin YX, Ma W, Zhang HJ, Chen KM, He GP, *et al*. Vasculogenic mimicry formation in EBV-associated epithelial malignancies. *Nat Commun* 2018; **9**:5009.
5 Mao XG, Xue XY, Wang L, Zhang X, Yan M, Tu YY, *et al*. CDH5 is specifically activated in glioblastoma stemlike cells and contributes to vasculogenic mimicry induced by hypoxia. *Neuro Oncol* 2013; **15**:865–879.
6 Huang H, He J, Johnson D, Wei Y, Liu Y, Wang S, *et al*. Deletion of placental growth factor prevents diabetic retinopathy and is associated with Akt activation and HIF1α-VEGF pathway inhibition. *Diabetes* 2015; **64**:200–212.
7 Ou M, Sun X, Liang J, Liu F, Wang L, Wu X, Tu J. A polysaccharide from Sargassum thunbergii inhibits angiogenesis via downregulating MMP-2 activity and VEGF/HIF-1α signaling. *Int J Biol Macromol* 2017; **94**:451–458.
8 Li YY, Zheng YL. Hypoxia promotes invasion of retinoblastoma cells *in vitro* by upregulating HIF-1α/MMP9 signaling pathway. *Eur Rev Med Pharmacol Sci* 2017; **21**:5361–5369.
9 Li S, Zhang Q, Zhou L, Guan Y, Chen S, Zhang Y, Han X. Inhibitory effects of compound DMBT on hypoxia-induced vasculogenic mimicry in human breast cancer. *Biomed Pharmacother* 2017; **96**:982–992.
10 Sun B, Zhang D, Zhang S, Zhang W, Guo H, Zhao X. Hypoxia influences vasculogenic mimicry channel formation and tumor invasion-related protein expression in melanoma. *Cancer Lett* 2007; **249**:188–197.
11 Chen S, Dong G, Wu S, Liu N, Zhang W, Sheng C. Novel fluorescent probes of 10-hydroxyevodiamine: autophagy and apoptosis-inducing anticancer mechanisms. *Acta Pharm Sin B* 2019; **9**:144–156.
12 Deng JD, Lei S, Jiang Y, Zhang HH, Hu XL, Wen HX, *et al*. A concise synthesis and biological study of evodiamine and its analogues. *Chem Commun (Camb)* 2019; **55**:3089–3092.
13 Shi L, Yang F, Luo F, Liu Y, Zhang F, Zou M, Liu Q. Evodiamine exerts anti-tumor effects against hepatocellular carcinoma through inhibiting β-catenin-mediated angiogenesis. *Tumour Biol* 2016; **37**:12791–12803.
14 Shyu KG, Lin S, Lee CC, Chen E, Lin LC, Wang BW, Tsai SC. Evodiamine inhibits *in vitro* angiogenesis: Implication for antitumorgenicity. *Life Sci* 2006; **78**:2234–2243.
15 Karroum A, Mirshahi P, Faussat AM, Therwath A, Mirshahi M, Hatmi M. Tubular network formation by adriamycin-resistant MCF-7 breast cancer cells is closely linked to MMP-9 and VEGFR-2/VEGFR-3 over-expressions. *Eur J Pharmacol* 2012; **685**:1–7.
16 Zhou P, Li XP, Jiang R, Chen Y, Lv XT, Guo XX, *et al*. Evodiamine inhibits migration and invasion by Sirt1-mediated post-translational modulations in colorectal cancer. *Anticancer Drugs* 2019; **30**:611–617.
17 Yang W, Gong X, Wang X, Huang C. A mediator of phosphorylated Smad2/3, evodiamine, in the reversion of TAF-induced EMT in normal colonic epithelial cells. *Invest New Drugs* 2019; **37**:865–875.
18 Hendrix MJ, Seftor EA, Meltzer PS, Gardner LM, Hess AR, Kirschmann DA, *et al*. Expression and functional significance of VE-cadherin in aggressive human melanoma cells: role in vasculogenic mimicry. *Proc Natl Acad Sci U S A* 2001; **98**:8018–8023.
19 Zang M, Hu L, Zhang B, Zhu Z, Li J, Zhu Z, *et al*. Luteolin suppresses angiogenesis and vasculogenic mimicry formation through inhibiting Notch1-VEGF signaling in gastric cancer. *Biochem Biophys Res Commun* 2017; **490**:913–919.
20 Hendrix MJ, Seftor EA, Hess AR, Seftor RE. Vasculogenic mimicry and tumour-cell plasticity: lessons from melanoma. *Nat Rev Cancer* 2003; **3**:411–421.
21 Gerri C, Marín-Juez R, Marass M, Marks A, Maischein HM, Stainier DYR. Hif-1α regulates macrophage-endothelial interactions during blood vessel development in zebrafish. *Nat Commun* 2017; **8**:15492.
22 Cheng G, Zhong M, Kawaguchi R, Kassai M, Al-Ubaidi M, Deng J, *et al*. Identification of PLXDC1 and PLXDC2 as the transmembrane receptors for the multifunctional factor PEDF. *Elife* 2014; **3**:e05401.
23 Orgaz JL, Ladhani O, Hoek KS, Fernández-Barral A, Mihic D, Aguilera O, *et al*. 'Loss of pigment epithelium-derived factor enables migration, invasion and metastatic spread of human melanoma'. *Oncogene* 2009; **28**:4147–4161.
24 Huang Z, Bao SD. Roles of main pro- and anti-angiogenic factors in tumor angiogenesis. *World J Gastroenterol* 2004; **10**:463–470.
25 Ribatti D. The discovery of antiangiogenic molecules: a historical review. *Curr Pharm Des* 2009; **15**:345–352.
26 Chen X, Zhang H, Zhu H, Yang X, Yang Y, Yang Y, *et al*. Endostatin combined with radiotherapy suppresses vasculogenic mimicry formation through inhibition of epithelial-mesenchymal transition in esophageal cancer. *Tumour Biol* 2016; **37**:4679–4688.
27 Ju J, Rastelli L, Malyanker UM, Simons JF, Huang C, Herrmann J, *et al*. The melanoma vascular mimicry phenotype defined in gene expression and microsome sequencing analysis. *Cancer Genomics Proteomics* 2004; **1**:355–362.